SUPPLEMENTAL DATA

Smad4 Loss Causes Spontaneous Head and Neck Cancer with Increased Genomic Instability and Inflammation

Sophia Bornstein, Ruth White, Stephen Malkoski, Masako Oka, Gangwen Han, Timothy Cleaver, Douglas Reh, Peter Anderson, Neil Gross, Susan Olson, Chuxia Deng, Shi-Long Lu, Xiao-Jing Wang

Supplemental Experimental Procedures

Mouse Strains. All animal experiments were performed using protocols approved by the IACUC at the Oregon Health & Science University and IACUC at the University of Colorado Denver. The inducible head-and-neck specific knockout system consists of two mouse lines, the *K14.CrePR1* or *K5.Cre*PR1* mice, in which Cre recombinase can be activated in head-and-neck epithelia by RU486 (1, 2), and the *Smad4f/f* mice, in which the *Smad4* gene is floxed (3). These mouse lines were crossbred to generate compound mice, allowing for homozygous *Smad4* deletion (Figure S1A). Littermates were genotyped at 3 weeks of age using primer pairs P9 and P10, and grouped based on genotypes for the experiments. RU486 (100 μl of 0.2μg/μl in sesame oil) was applied in the oral cavity of 4-week-old bigenic mice daily for 5 consecutive days to induce homozygous deletion of the *Smad4* gene. Monogenic (*K14.CrePR1*, *K5.Cre*PR1*, or *Smad4f/f)* control littermates were treated with the same RU486 regimen as bigenic mice. To generate control tumors, we utilized an RU486-inducible *K15.CrePR1 line* (4) in combination with a knock-in mutant $Kras^{G12D}$ allele (5) to generate $K15.CrePR1/Kras^{G12D}$ mice. We also mated these mice to *Smad4f/f* mice to generate

K15.CrePR1/Kras^{G12D}*/Smad4f/w* mice. The *K15* promoter also targets *CrePR1* expression to head-and-neck epithelia. To generate *Smad4f/f/Smad3+/-* mice for inflammation studies, we mated *K14.CrePR1/Smad4f/f* or *K5.Cre*PR1/Smad4f/f* mice with our previously described germline *Smad3+/-* mice (7) and RU486 was applied to 3-week-old mice using the same regimes described above. The general condition of the mice was checked at least once per week prior to the development of visible tumors. Mice with oral tumors were given soft food and monitored daily. Tumor-bearing mice were euthanized when oral tumors became ulcerated, or at the first sign of deteriorating health or pain resulting from tumors (e.g., huddled posture, vocalization, hypothermia, or ≥20% weight loss). Paired *HN-Smad4+/+* littermates were euthanized at the same time and the corresponding tissue samples were dissected as controls. Necropsy was performed on each euthanized mouse to identify primary tumors and distant metastases. To dissect early preneoplastic lesions, mice with each genotype were euthanized at 4 weeks after *Smad4* deletion, and head-and-neck tissue including the buccal tissue, tongue, esophagus, and forestomach were dissected.

Characterization of Head-and-Neck Epithelia-Specific Smad4 Knockout Mice. To verify *Smad4* deletion in the head-and-neck epithelia, we euthanized *K5.Cre*PR1/Smad4f/f* or *K14.CrePR1/Smad4f/f* bigenic mice and monogenic control mice 10 days after the final RU486 treatment and extracted DNA from buccal mucosa, tongue, and esophagus. The recombinant *Smad4* allele lacking exon 8 was readily detected in the above tissues by PCR in *K5.Cre*PR1/Smad4f/f* and *K14.CrePR1/Smad4f/f* bigenic mice, but not monogenic control littermates, using primer pairs P8 and P10 (Figure S1B).

*Loss of Heterozygosity (LOH).*DNA was extracted and PCR amplified using FAM-labeled forward primers for microsatellite markers adjacent to the Smad4 gene. PCR products were column purified (Promega) and analyzed using fragment length polymorphism analysis (ABI) at the OHSU MMI sequencing core to determine the size of Smad4 alleles. Two PCR products (peaks) indicated a heterozygous sample, while one product indicated a homozygous sample. LOH for a given marker was positive if the following calculation: (peak height of allele 1 of tumor/peak height of allele 2 of tumor) compared to (peak height of allele 1 of adjacent mucosa/peak height of allele 2 of adjacent mucosa) was greater than or equal to 1.5. LOH for the Smad4 locus was considered positive if either of the flanking microsatellite markers exhibited LOH. Sequences: D18S46: FAM-GAATAGCAGGACCTATCAAAGAGC, CAGATTAAGTGAAAACAGCATATGTG; D18S474: FAM-TGGGGTGTTTACCAGCATC, TGGCTTTCAATGTCAGAAGG.

Ras Sequencing. Genomic DNA was extracted from samples as previously described (8) and sequenced with the following primers:

Hras Exon 1 forward primer: GCAGCCGCTGTAGAAGCTATGA

Hras Exon 1 reverse primer: GTAGGCAGAGCTCACCTCTATA

Hras Exon 2 forward primer: CATGACTGTGTCCAGGACATTC

Hras Exon 2 reverse primer: TAGGCTGGTTCTGTGGATTCTC

Kras Exon 1 forward primer: TACACACAAAGGTGAGTGTAAAAATATTGATAA

Kras Exon 1 reverse primer: AGAGCAGCGTTACCTCTATC

Kras Exon 2 forward primer: AAGATGCACTGTAATAATCCATAC

Kras Exon 2 reverse primer: ATTCAACTTAAACCCACCTATA

Sequences were uploaded and mutations were detected using Chromas Lite software.

TUNEL Staining. Immunoflurorescence of Tdt-mediated dUTP Nick-End Labeling (TUNEL) assays was performed using the TUNEL assay kit (Promega).

Western Blotting. Protein was extracted from cells as previously described (9) and Western blotting was performed using primary antibodies to both Smad4 and Actin (Santa Cruz). The blot was then incubated with Alexa Fluor 700 secondary antibody to detect Smad4 and Alexa Fluor 800 secondary antibody to detect Actin (Molecular Probes), and scanned with the Odyssey Infrared Imaging System (LI-COR Biosciences).

Supplemental Figure Legends

Figure S1. Loss of heterozygosity (LOH) at the Smad4 locus occurred in 33% (6/18) of adjacent mucosa and HNSCC pairs analyzed. **(A)** 18 matched sample pairs of HNSCC and adjacent mucosa with case numbers at the top corresponding to samples from Figure 1A are displayed, and microsatellite markers used for PCR flanking the Smad4 locus are listed on the left side (D18S474, D18S46). Markers showing LOH, retention of heterozygosity, or that were homozygous in the adjacent mucosa sample (not informative) are displayed. *: samples exhibiting LOH in a microsatellite marker adjacent to Smad4. **(B)** Representative histograms of a heterozygous normal adjacent sample with paired HNSCC exhibiting loss of heterozygosity (indicated by an arrow), for both flaking microsatellite markers used (D18S474, D18S46).

Figure S2. Smad4 was deleted in head-and-neck epithelia. A: Schematic of mating strategy to generate bigenic *K5.Cre*PR1.Smad4f/f* or *K14.CrePR1.Smad4f/f* mice. B: An example of *Smad4* genotyping PCR using primers 9 and 10 ("WT" indicates the wild-type *Smad4* allele), and detection of the recombinant allele with deleted exon 8 in bigenic mice, using deletion-specific PCR with primers 8 and 10. C: Relative expression of Smad4 transcripts examined by quantitative RT-PCR (qRT-PCR). Smad4 expression was lost in *HN-Smad4-/-* mucosa and HNSCC. Residual expression in these tissues is due to contaminating stromal cells that retain expression of Smad4. The average expression from 5-10 samples in each group are presented. The average expression of Smad4 in the *HN-Smad4+/+* samples was arbitrarily set to 100%. Error bars indicate SE. Significance was calculated using a student's *t*-test: * = $p<0.05$ in comparison with *HN-Smad4+/+* mucosa. D: IHC of Smad4 in mouse buccal tissue and HNSCC. Note that the Smad4 protein was detected in the buccal epithelia of a *HN-Smad4+/+* mouse orally treated with RU486. Smad4 was specifically ablated in the buccal mucosa of a *HN-Smad4-/-* mouse treated orally with RU486, and an HNSCC arising from a *HN-Smad4-/-* mouse. 5-10 samples from each group were examined and a representative picture is presented. The scale bar in the top panel represents 40 μm for all panels.

Figure S3. HN-Smad4-/- HNSCC exhibited increased proliferation and reduced apoptosis. A: PCNA staining of *HN-Smad4+/+* mucosa, *HN-Smad4-/-* mucosa, and *HN-Smad4-/-* HNSCC. *HN-Smad4-/-* mucosa had increased proliferation compared to *HN-Smad4+/+* mucosa, and proliferation was further increased in *HN-Smad4-/-* HNSCC. 5-

10 samples were analyzed and a representative picture is presented. B: TUNEL staining of *HN-Smad4+/+* mucosa, *HN-Smad4-/-* mucosa, and *HN-Smad4-/-* HNSCC. Apoptosis was reduced in *HN-Smad4-/-* mucosa compared to *HN-Smad4+/+* mucosa, and further reduced in *HN-Smad4-/-* HNSCC. 5-10 samples were analyzed and a representative picture is presented. The scale bar in the upper left panel represents 20 μm for all panels.

Figure S4. Ras activation cooperates with Smad4 in HNSCC tumorigenesis. A: *H-ras* sequencing traces in *HN-Smad4-/-* HNSCC revealed spontaneous codon 61 mutations in 4/18 cases. Examples of each type of mutation (CAA to CAC, CTA, or CGA) are presented. B: IHC for Ras revealed that Ras proteins were overexpressed in *HN-Smad4-/-* mucosa and HNSCC compared to *HN-Smad4+/+* mucosa. C: H&E staining of *HN-K-ras*^{G12D}*/Smad4+/-* dyspastic mucosa and HNSCC sections. The scale bar in the top panel of B represents 40 μm for all panels in B and C.

Figure S5. Smad4 Knockdown in Normal Keratinocytes and Restoration in Smad4-deficient HNSCC cells. qRT-PCR and Western analysis of Smad4 levels in HEKn, HEKn + Smad4 siRNA, Cal27, and Cal27-Smad4 cells. The qRT-PCR values were calculated relative to HEKn cells arbitrarily set at 100% for every experiment. Samples were run in triplicate for each experiment, and the average relative expression levels from 3-4 pooled experiments are presented. *: $p<0.05$ for HEKn + Smad4 siRNA compared to HEKn cells, and †: $p<0.05$ for Cal27-Smad4 cells compared to Cal27 cells. Western blotting for Smad4 revealed that Smad4 was lost at the protein level by over 70% in HEKn + Smad4 siRNA compared to HEKn cells, and restored in Cal27-Smad4 compared to Cal27 cells.

Figure S1

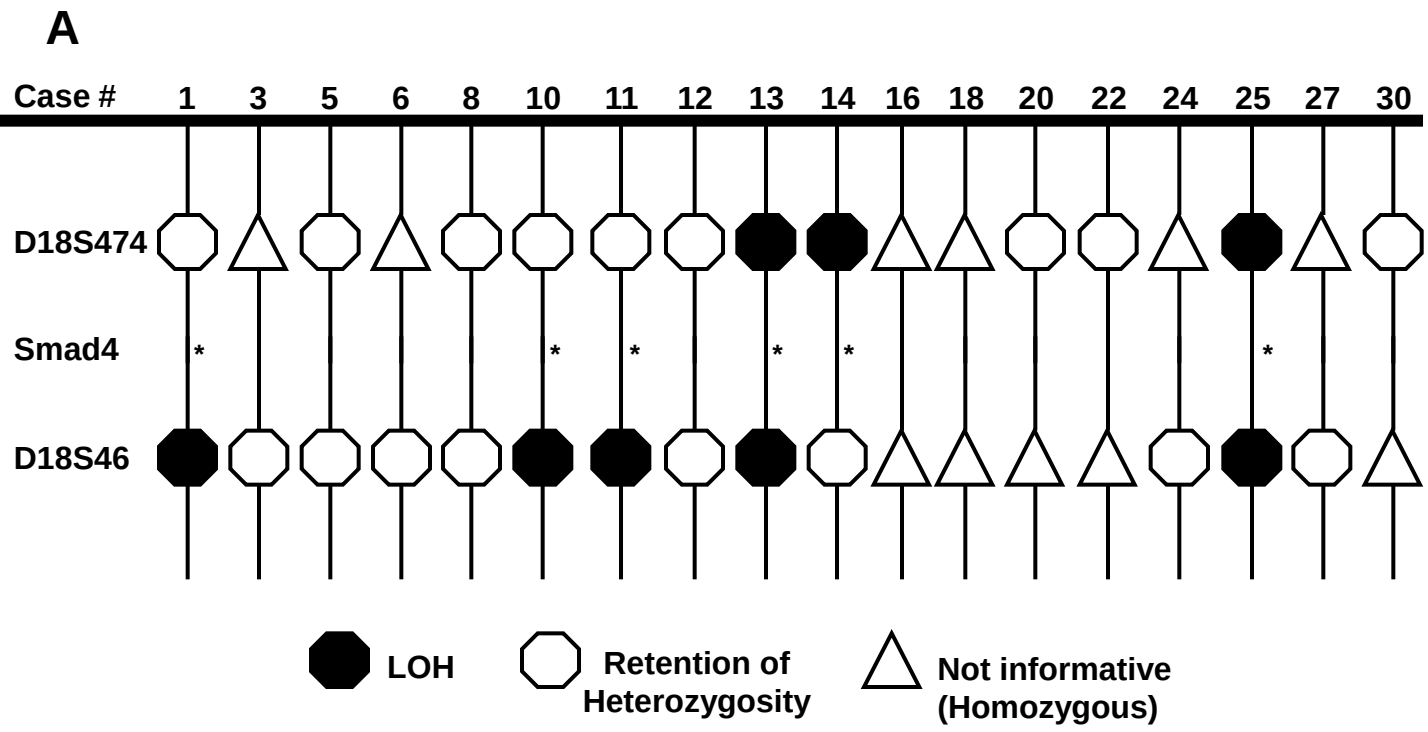
A
Case #
1
3
5
6
8
10
11
12
13
14
16
18
20
22
24
25
27
30
D18S474
Smad4
D18S46
LOH
Retention of Heterozygosity
Not informative (Homozygous)

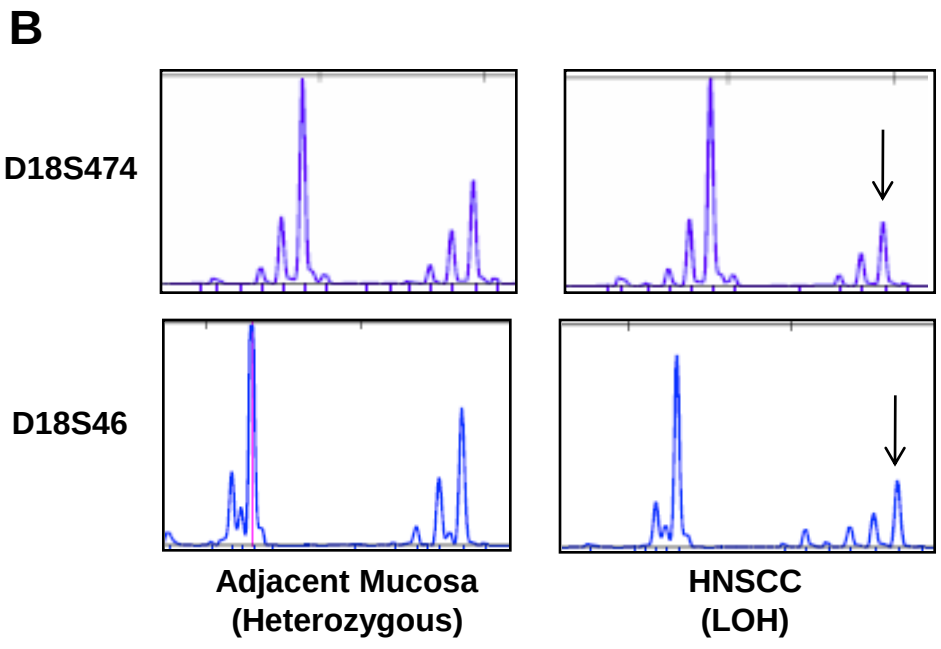
B
D18S474
D18S46
Adjacent Mucosa (Heterozygous)
HNSCC (LOH)

Figure S2

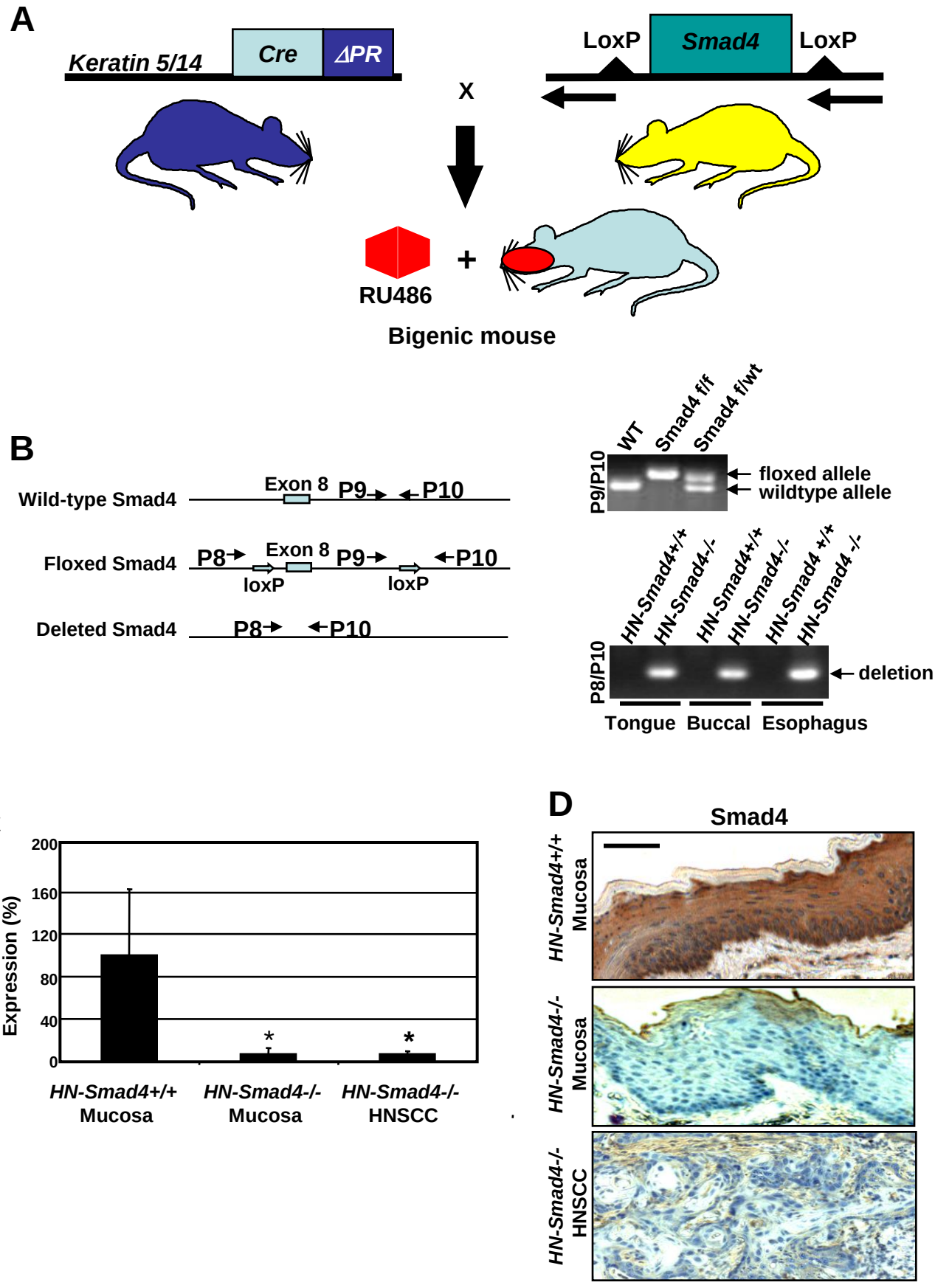
A
Keratin 5/14
Cre
ΔPR
X
LoxP
Smad4
LoxP
RU486
+
Bigenic mouse
B
Wild-type Smad4
Exon 8
P9
P10
Floxed Smad4
P8
Exon 8
P9
P10
loxP
loxP
Deleted Smad4
P8
P10
WT
Smad4 f/f
Smad4 f/wt
P9/P10
floxed allele
wildtype allele
HN-Smad4+/+
HN-Smad4-/-
HN-Smad4+/+
HN-Smad4-/-
HN-Smad4 +/+
HN-Smad4 -/-
P8/P10
deletion
Tongue
Buccal
Esophagus
C
Smad4 Relative mRNA Expression (%)
200
160
120
80
40
0
*
*
HN-Smad4+/+ Mucosa
HN-Smad4-/- Mucosa
HN-Smad4-/- HNSCC
D
Smad4
HN-Smad4+/+ Mucosa
HN-Smad4-/- Mucosa
HN-Smad4-/- HNSCC

Figure S3

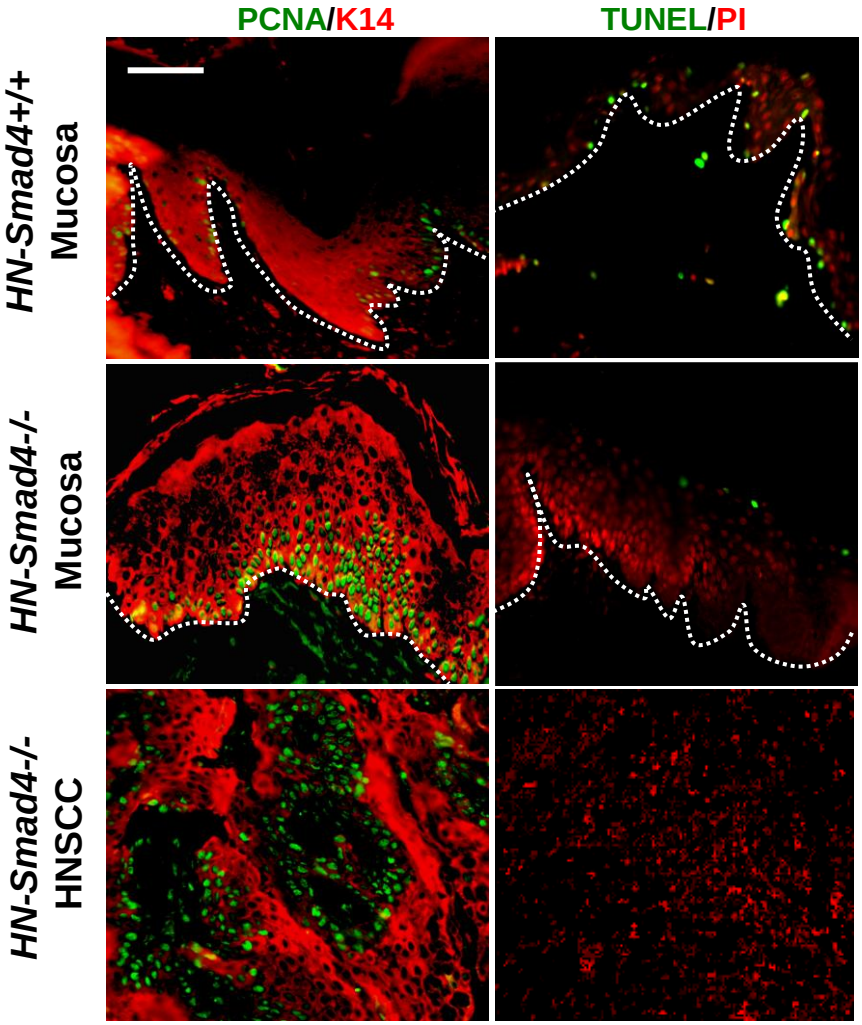
PCNA/K14
TUNEL/PI
HN-Smad4+/+ Mucosa
HN-Smad4-/- Mucosa
HN-Smad4-/- HNSCC

Figure S4

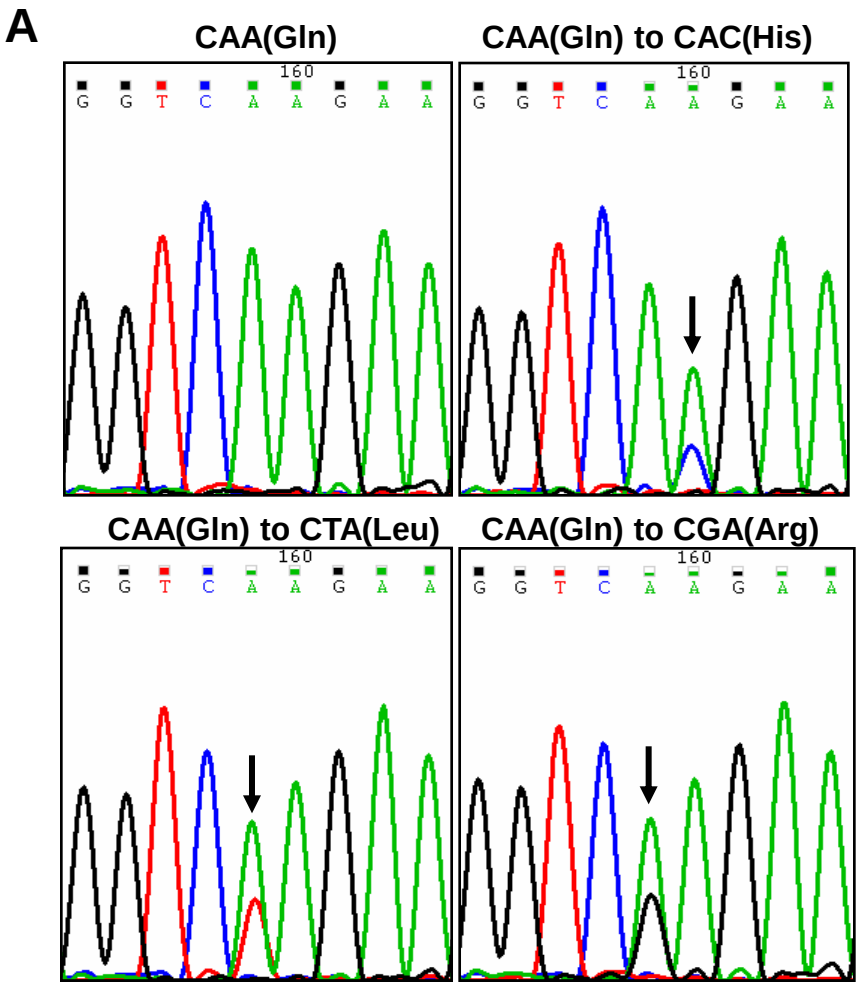
A
CAA(Gln)
CAA(Gln) to CAC(His)
CAA(Gln) to CTA(Leu)
CAA(Gln) to CGA(Arg)
160
G G T C A A G A A

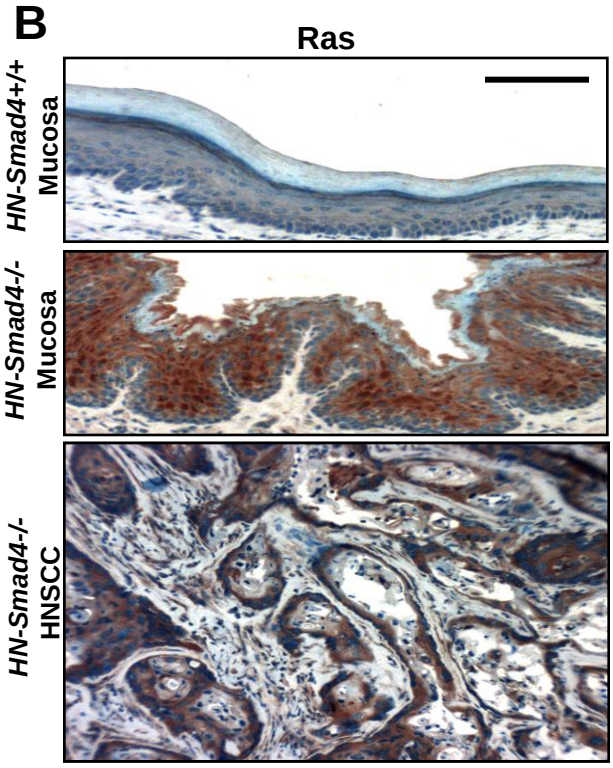
B
Ras
HN-Smad4+/+ Mucosa
HN-Smad4-/- Mucosa
HN-Smad4-/- HNSCC

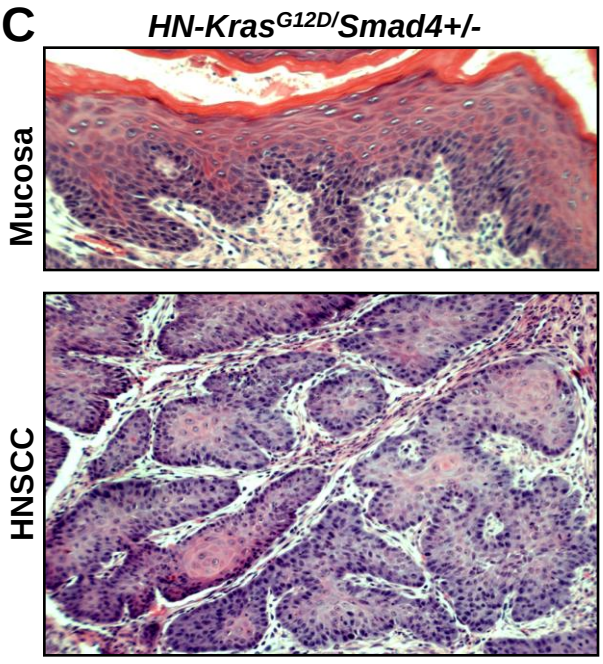
C
HN-KrasG12D/Smad4+/-
Mucosa
HNSCC

Figure S5

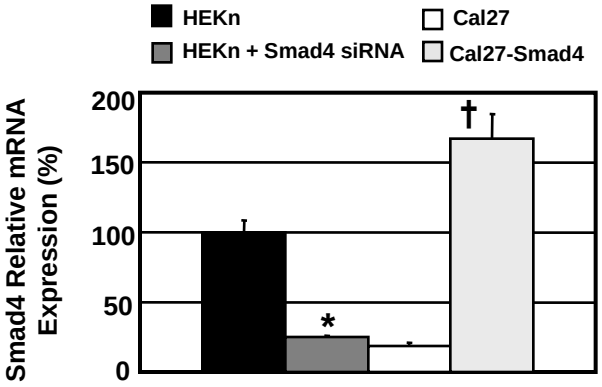
HEKn
HEKn + Smad4 siRNA
Cal27
Cal27-Smad4
Smad4 Relative mRNA Expression (%)
200
150
100
50
0
*
†

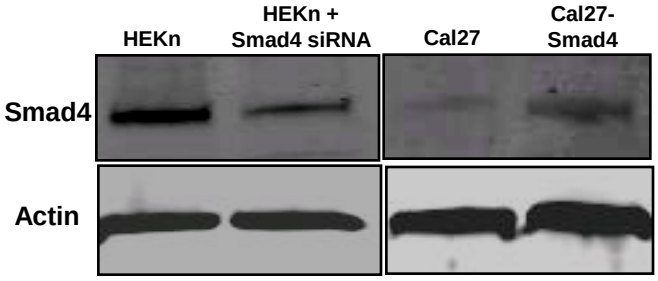
HEKn
HEKn + Smad4 siRNA
Cal27
Cal27-Smad4
Smad4
Actin

Supplemental References

1. Berton, T.R., Wang, X.J., Zhou, Z., Kellendonk, C., Schutz, G., Tsai, S., and Roop, D.R. 2000. Characterization of an inducible, epidermal-specific knockout system: differential expression of lacZ in different Cre reporter mouse strains. *Genesis* 26:160-161.
2. Caulin, C., Nguyen, T., Longley, M.A., Zhou, Z., Wang, X.J., and Roop, D.R. 2004. Inducible activation of oncogenic K-ras results in tumor formation in the oral cavity. *Cancer Res* 64:5054-5058.
3. Yang, X., Li, C., Herrera, P.L., and Deng, C.X. 2002. Generation of Smad4/Dpc4 conditional knockout mice. *Genesis* 32:80-81.
4. Morris, R.J., Liu, Y., Marles, L., Yang, Z., Trempus, C., Li, S., Lin, J.S., Sawicki, J.A., and Cotsarelis, G. 2004. Capturing and profiling adult hair follicle stem cells. *Nat Biotechnol* 22:411-417.
5. Jackson, E.L., Willis, N., Mercer, K., Bronson, R.T., Crowley, D., Montoya, R., Jacks, T., and Tuveson, D.A. 2001. Analysis of lung tumor initiation and progression using conditional expression of oncogenic K-ras. *Genes Dev* 15:3243-3248.
6. Lu, S.L., Reh, D., Li, A.G., Woods, J., Corless, C.L., Kulesz-Martin, M., and Wang, X.J. 2004. Overexpression of transforming growth factor beta1 in head and neck epithelia results in inflammation, angiogenesis, and epithelial hyperproliferation. *Cancer Res* 64:4405-4410.
7. Li, A.G., Lu, S.L., Zhang, M.X., Deng, C., and Wang, X.J. 2004. Smad3 knockout mice exhibit a resistance to skin chemical carcinogenesis. *Cancer Res* 64:7836-7845.
8. Lu, S.L., Herrington, H., Reh, D., Weber, S., Bornstein, S., Wang, D., Li, A.G., Tang, C.F., Siddiqui, Y., Nord, J., et al. 2006. Loss of transforming growth factor-beta type II receptor promotes metastatic head-and-neck squamous cell carcinoma. *Genes Dev* 20:1331-1342.
9. Li, A.G., Wang, D., Feng, X.H., and Wang, X.J. 2004. Latent TGFbeta1 overexpression in keratinocytes results in a severe psoriasis-like skin disorder. *Embo J* 23:1770-1781.